PHOTOSYSTEM I FROM HIGHER PLANTS ENHANCES ELECTRODE PERFORMANCE

By

Darlene Gunther

Thesis

Submitted to the Faculty of the

Graduate School of Vanderbilt University

in partial fulfillment of the requirements

for the degree of

Master of Science

in

Interdisciplinary Materials Science

May, 2013

Nashville, Tennessee

Approved:

Professor G. Kane Jennings

Professor David E. Cliffel

ACKNOWLEDGEMENTS

No great works represent the work of one person, for each individual has been privileged to receive instruction from the many individuals whom they have encountered throughout their life. As such, I am very grateful to God and his servants for bringing me to this point in my life. It is an honor for me to thank my advisor G. Kane Jennings for the many enlightening discussions and sound advice offered to direct me in my research and writing evolution. I am also honored to thank my co-advisor David E. Cliffel whose expertise has been critical in this work. I would like to thank Norman Tolk and Sharon Weiss for their academic support in solidifying my studies and sharing their valuable time with me. None of this would have been possible without the support of Richard Mu who has consistently encouraged me throughout graduate school. I would like to thank him for his contributions of time and resources to this project in particular and my education in general. His work provided the original inspiration for my graduate education. His contributions are too numerous to mention individually. Thank you, Dr. Mu. This thesis would not have been possible without the patient tutoring provided by Gabriel LeBlanc and Gongping Chen, as well as those of my colleague, Carlos Escobar. Additional contributions from Jaime Zhang, Karla Dumeng, Will Crosby, and Dhiraj Prasai made this work possible. Professor Kirill Bolotin's expertise provided the foundation for the exploration of graphene as a transparent, conducting electrode.

I would like to thank Kay Dayton from Volunteer State Community College in Gallatin, TN for her amazing talent in recognizing my potential and encouraging me to continue my education. She is perhaps the first career mentor in my life. I thank her for the many conversations we have shared and her tremendous gift to mentor.

I would like to acknowledge the contributions of my two sisters, Gail G. Phillips and Jo Ann Glover. These two remarkable women are quite successful in their own right and have provided me continuous emotional support and encouragement throughout my educational process. One of three girls, I am the first of the Gunther sisters to acquire a college degree. This is not because of intelligence but rather upbringing. We were taught that an education is wasted on a woman. So I am very grateful to God that I have been allowed to transcend that erroneous message and by His Grace, obtain the Masters of Science degree to which this thesis belongs. I am grateful to my Mother for many qualities she imparted to me, particularly determination and goal setting. I am sorry she was not able to enjoy this accomplishment in my life. Similarly, my Father passed on many years ago but he had such a positive influence in my life that any accomplishment remiss of acknowledging him would be a disgrace. So I thank my father, James Gunther for giving me so much more than words can convey.

Finally, I am truly grateful for the financial support provided by EPA (SU8360221) and NSF (DMR 0907619 and EPS 1004083)Original funding for this project was provided by the USDA-CSREES (2005-35603-15303) and a Vanderbilt University Discovery grant. In addition, this research was supported in part by the Scialog program from the Research Corporation for Science Advancement.

TABLE OF CONTENTS

LIST OF FIGURES

ABBREVIATIONS

Å – angstrom

Ag/AgCl – silver/silver chloride

Au – gold

Chl *a* – chlorophyll *a*

Chl *b* – chlorophyll *b*

Cu – copper

DTT – dithiothreitol (Cleland's Reagent)

H_2O – water

HF – hydrofluoric acid

IR – infra-red

KCl – potassium chloride

kDa – kilo Dalton

L – liter

M – Molarity

MB – methylene blue

mmol/ml – millimol per milliliter

MV – methyl viologen

N_2 – nitrogen

NaCl – sodium chloride

NaOH – sodium hydroxide

nm – nanometer

nmol/mL – nanomol per milliliter

p-Si – positively-doped silicon

PSI – photosystem I

Pt – platinum

RuHex – ruthenium hexamine trichloride

Sccm – standard cubic centimeter

SiO_2 – silicon dioxide

UV-vis – ultraviolet visible

μm – micrometer

CHAPTER I

Introduction

Photosystem I (PSI), a supramolecular protein complex found within the thylakoid membrane of higher plants, some algae, and cyanobacteria, drives nature's 90-terawatt solar energy conversion process known as photosynthesis. Higher plants are members of the Plantae kingdom, distinguished by their vascular tissues, which circulate resources throughout the plant. The most striking and important feature of these plants is their green color, which is the result of pigments known as chlorophyll.[1] Special groups of chlorophylls, designated as chlorophyll *a* (chl *a*),[2] are responsible for light harvesting: transforming the energy absorbed from the sun to molecules that convert the sunlight into chemical energy that it can store or use to produce food (photosynthesis). Not surprisingly, these chl *a* molecules are often referred to as antennae complexes.

PSI uses this system of chlorophylls to harvest incident photons[·] and transfer their energy to a special pair of chlorophylls known as P_{700}. Upon receipt of the incident energy (photon) by the P_{700} reaction dimer, rapid charge separation occurs (within 10-30 ps),[3] releasing an electron down an intra-protein energy cascade to an iron-sulfur complex called F_B. In nature, the soluble, iron-containing protein ferredoxin shuttles the electrons away from F_B^- to achieve a nearly perfect quantum yield.[4] This remarkable photocatalytic functionality, PSI's nanometer size, and its

[·] Photon: a particle representing a quantum of light or electromagnetic radiation.

vast abundance have encouraged researchers to incorporate PSI into biohybrid structures, with many successes reported over the past decade.[5,6,7,8]

Optimization of these systems continues to be a challenge. The visible light energy conversion efficiency is 47% (~23% for the solar spectrum).[9] Device efficiencies as discussed by Ciesielski et al.[8] relative to a photoelectrochemical 'wet' cell, remain limited due to mediator diffusion constraints. In order to approach quantum efficiencies of 10% or more it is necessary to optimize mediator (electrolyte) solutions in these 'wet' cells, removing mass transfer barriers such as mediator diffusion. One means of improving the diffusion limitation would be to increase the concentration of electrolyte in these systems. However, this creates another problem. As mediator concentration increases, the mediator solution can become opaque. An opaque mediator would greatly limit light penetration to the active electrode, resulting in decreased efficiency. Solving this problem would benefit photoelectrochemical cells and possibly the semiconductor nanoparticle-based dye-sensitized solar cells as well.

Since the pioneering work reporting the extraction of graphene from bulk graphite via micromechanical exfoliation,[10] improvements in synthesis and characterization methods for graphene have provided the opportunity to exploit this novel material as a transparent, highly conductive electrode,[11] opening a window of opportunity for increased mediator concentration. Graphene sheets are two-dimensional layers of sp^2 hybridized carbon atoms, which have interesting and unique properties such as high carrier mobility,[12] high elasticity and breaking strength,[13] record thermal conductivity (~3000 W/m-K in plane)[14] and high

transparency over the visible spectrum (97.7%).[15] These extraordinary electronic, mechanical, and optical properties of graphene are inviting for applications from solar cells to transistors.[16] By combining the unique photodiode properties of PSI with the exceptional optical and electronic properties of graphene, I will herein establish the foundation for integration of these ultrathin materials into a new photoactive electrode. Furthermore, I will investigate opaque mediators with this system, which I hypothesize will provide increased photocurrents.

For over a decade, scientists have been applying their skills to solving the global energy crisis with a concentrated focus on renewable energy. Photosystem I represents an incredibly abundant source of renewable energy. It is available in all the higher plants. Extraction of PSI from plants comes predominantly from spinach in current research, which the critics point out is a food source. If one drives practically anywhere in the southern United States of America, it is highly probable that massive vine growth will be noticeable along the interstate as well as throughout rural state highways. These are the kudzu vines (*Pueraria lobata).* Figure 1 shows the invasive nature of this plant as it grows over a street lamp and local ground cover vegetation. Symbolically in this picture, it appears human and can metaphorically be labeled as the Queen of the plant kingdom in this region.

Kudzu is a rapidly growing vine covering in excess of 810,000 hectare (ha) of the southern United States of America.[17] It is a member of the pea family, *Leguminosae* and was introduced into the U.S. as a soil stabilizer, animal food, and

Figure 1. *Pueraria lobata* (kudzu) vines overtaking a streetlight in rural America, courtesy of http://www.firehow.com/201002259293/how-to-plant-and-grow-kudzu.html

ornamental vine in 1876.[17] As many consider the vine a nuisance, it is surprising to learn of its commercial appeal. Kudzu is used as a cooking starch, a natural medicine, fibers for weaving and paper production, a source for methane and gasohol,[17] a supplement for existing bioethanol feedstock,[18] and a food for ruminants.[19] Unfortunately, kudzu has a devastatingly negative impact in the southern United States where it quickly overtakes local vegetation, crops and forest. In 2009, Sage et al.[18] stated that kudzu cost the US economy over $500 million per year as lost crops and forest productivity, expenditures for control, and damage to property. Approaches to eradicate this pesky weed are expensive, challenging, and potentially harmful to the environment. Studies suggest the eradication of established kudzu areas require multiple years of applied herbicides and alternative plantings.[17,19] Due to the extensive problems associated with this vine, the U.S. Congress placed kudzu on the list of federal noxious weeds in July of 1997.[17,19], Motivating commercial applications for this vine is a prudent strategy for controlling its growth. One such opportunity is to isolate the PSI protein complexes

found in its leaves. An important question to consider is this, "Is PSI from kudzu homologous to PSI from spinach?"

In 1974, Shiozawa et al.[20] extracted PSI from several plants in order to compare and contrast them with those from blue-green algae. These included tobacco (*Nicotiana tabacum*), jack bean *(Canavalia ensiformis (L.) (DC.))*, bush bean *(Phaseolus vulgaris)*, peas *(Pisum sativa)*, barley *(Hordeum vulgare)*, corn *(Zea mays)*, and pine needles (*Pinus radiate)* from mature trees. Their analysis found a slight shift in the spectral absorption peaks of PSI, from 677 nm in algal moiety to 671 nm in the higher plant. Otherwise, no differences were identified between higher-plant PSI and blue-green algae PSI. The authors concluded that the PSI complex is homologous in higher plants and differs from blue-green algae due to the presence of chl *b*, which is absent from algae extractions.

Twenty-seven years later (2001), Scheller et al.[21] published an in-depth review/discussion of the subunits in eukaryotic PSI, identifying differences found between plant and algae PSI complexes. The review concludes that eukaryotic PSI is now relatively well understood.

Shiozawa's et al.[20] work also presented an improved isolation/extraction method for PSI complexes with the added benefit of improved kinetics. Importantly this work attributes variable results in the literature to variations in the extraction process. Still others have extracted PSI from barley,[22] swiss chard,[23] lettuce and quinoa[24]. In the latter case, Reeves and Hall studied the activity of isolated chloroplast relative to electron transport. The study noted that "high activity is not easy" as demonstrated by data from spinach PSI, which has fluctuations due to

seasonal variations.[24] The primary focus of the article was to standardize the extraction process, which can have a negative effect on the resultant fraction, relative to kinetics and photo activity of the extracted PSI.

These studies are of interest to the work herein. Collectively the studies find that PSI from higher plants is homologous. This work includes extractions from two higher plant varieties, spinach and kudzu, following the Reeves and Hall optimization for extraction processes discussed above, with slight modifications (see chapter II). In the analysis of PSI from kudzu and spinach leaves used in this work, the concentration of kudzu PSI measured an order of magnitude lower than the concentration of spinach PSI, even though the process of extraction was the same. This generates the question of PSI concentration in the different species and provides opportunities for future studies with kudzu.

Recently, our group addressed the issue of PSI orientation relative to metal substrates by selecting boron-doped (p-Si) silicon semiconductor as the substrate.[25] Through band-gap alignment, unidirectional electron flow occurs into the PSI film eliminating the necessity of aligning each PSI upon the substrate. That system provided a 2500-fold enhancement over PSI on planar gold substrates under identical testing. Consequently, this system was chosen for testing PSI from kudzu leaves. The work herein reports on the successful extraction of PSI from kudzu leaves and deposited onto p-Si to enhance photoelectrochemical energy conversion over p-Si alone.

References:

1. Introduction to the Plantae. http://www.ucmp.berkeley.edu/plants/plantae.html.
2. Porra, R. J., The chequered history of the development and use of simultaneous equations for the accurate determination of chlorophylls a and b. *Photosynthesis Research* **2002,** *73* (1-3), 149-156.
3. Chitnis, P. R., Photosystem I: Function and physiology. *Annual Review of Plant Physiology and Plant Molecular Biology* **2001,** *52*, 593-626.
4. Golbeck, J. H., Structure and Function of Photosystem I. *Annual Review of Plant Physiology and Plant Molecular Biology* **1992,** *43* (1), 293-324.
5. Das, R.; Kiley, P. J.; Segal, M.; Norville, J.; Yu, A. A.; Wang, L.; Trammell, S. A.; Reddick, L. E.; Kumar, R.; Stellacci, F.; Lebedev, N.; Schnur, J.; Bruce, B. D.; Zhang, S.; Baldo, M., Integration of Photosynthetic Protein Molecular Complexes in Solid-State Electronic Devices. *Nano Letters* **2004,** *4* (6), 1079-1083.
6. Carmeli, I.; Frolov, L.; Carmeli, C.; Richter, S., Photovoltaic Activity of Photosystem I-Based Self-Assembled Monolayer. *Journal of the American Chemical Society* **2007,** *129* (41), 12352-12353.
7. Mershin, A.; Matsumoto, K.; Kaiser, L.; Yu, D. Y.; Vaughn, M.; Nazeeruddin, M. K.; Bruce, B. D.; Graetzel, M.; Zhang, S. G., Self-assembled photosystem-I biophotovoltaics on nanostructured TiO2 and ZnO. *Sci Rep-Uk* **2012,** *2*, 234-240.
8. Ciesielski, P. N.; Hijazi, F. M.; Scott, A. M.; Faulkner, C. J.; Beard, L.; Emmett, K.; Rosenthal, S. J.; Cliffel, D.; Kane Jennings, G., Photosystem I - Based biohybrid photoelectrochemical cells. *Bioresource Technology* **2010,** *101* (9), 3047-3053.
9. Toporik, H.; Carmeli, I.; Volotsenko, I.; Molotskii, M.; Rosenwaks, Y.; Carmeli, C.; Nelson, N., Large Photovoltages Generated by Plant Photosystem I Crystals. *Adv Mater* **2012,** *24* (22), 2988-2991.
10. Dreyer, D. R.; Ruoff, R. S.; Bielawski, C. W., From Conception to Realization: An Historial Account of Graphene and Some Perspectives for Its Future. *Angewandte Chemie International Edition* **2010,** *49* (49), 9336-9344.
11. Li, W.; Tan, C.; Lowe, M. A.; Abruna, H. D.; Ralph, D. C., Electrochemistry of Individual Monolayer Graphene Sheets. *ACS Nano* **2011,** *5* (3), 2264-2270.
12. Bolotin, K. I.; Sikes, K. J.; Jiang, Z.; Klima, M.; Fudenberg, G.; Hone, J.; Kim, P.; Stormer, H. L., Ultrahigh electron mobility in suspended graphene. *Solid State Commun.* **2008,** *146* (9,Äì10), 351-355.
13. Lee, C.; Wei, X. D.; Kysar, J. W.; Hone, J., Measurement of the elastic properties and intrinsic strength of monolayer graphene. *Science* **2008,** *321* (5887), 385-388.
14. Seol, J. H.; Jo, I.; Moore, A. L.; Lindsay, L.; Aitken, Z. H.; Pettes, M. T.; Li, X.; Yao, Z.; Huang, R.; Broido, D.; Mingo, N.; Ruoff, R. S.; Shi, L., Two-Dimensional Phonon Transport in Supported Graphene. *Science* **2010,** *328* (5975), 213-216.
15. Nair, R. R.; Blake, P.; Grigorenko, A. N.; Novoselov, K. S.; Booth, T. J.; Stauber, T.; Peres, N. M. R.; Geim, A. K., Fine Structure Constant Defines Visual Transparency of Graphene. *Science* **2008,** *320* (5881), 1308.
16. Celebrating Graphene. *Nature Photonics* **2010,** *4* (11), 731.
17. Mitich, L. W., Kudzu [Pueraria lobata (Willd.) Ohwi]. *Weed Technology* **2000,** *14* (1 (Jan.-March)), 231-235.
18. Sage, R. F.; Coiner, H. A.; Way, D. A.; Runion, G. B.; Prior, S. A.; Torbert, H. A.; Sicher, R.; Ziska, L., Kudzu [Pueraria montana (Lour.) Merr. Variety lobata]: A new source of carbohydrate for bioethanol production. *Biomass and Bioenergy* **2009,** *33*, 57-61.
19. Harrington, T. B.; Rader-Dixon, L. T.; Taylor, J. W., Kudzu (Pueraria montana) community responses to herbicides, burning, and high-density loblolly pine. *Weed Science* **2003,** *51* (6), 965-974.
20. Shiozawa, J. A.; Alberte, R. S.; Thornber, J. P., The P700-chlorophyll a-protein : Isolation and some characteristics of the complex in higher plants. *Archives of Biochemistry and Biophysics* **1974,** *165* (1), 388-397.

21. Scheller, H. V.; Jensen, P. E.; Haldrup, A.; Lunde, C.; Knoetzel, J., Role of subunits in eukaryotic Photosystem I. *Bba-Bioenergetics* **2001,** *1507* (1-3), 41-60.
22. Hiller, R. G.; Pilger, T. B. G.; Genge, S., Effect of Lincomycin on Chlorophyll Protein Complex-I Content and Photosystem-I Activity of Greening Leaves. *Biochim Biophys Acta* **1977,** *460* (3), 431-444.
23. Bengis, C.; Nelson, N., Purification and Properties of Photosystem-I Reaction Center from Chloroplasts. *J Biol Chem* **1975,** *250* (8), 2783-2788.
24. Reeves, S. G.; Hall, D. O., [8] Higher plant chloroplasts and grana: General preparative procedures (excluding high carbon dioxide fixation ability chloroplasts). In *Methods in Enzymology*, Anthony San, P., Ed. Academic Press: 1980; Vol. Volume 69, pp 85-94.
25. LeBlanc, G.; Chen, G. P.; Gizzie, E. A.; Jennings, G. K.; Cliffel, D. E., Enhanced Photocurrents of Photosystem I Films on p-Doped Silicon. *Adv Mater* **2012,** *24* (44), 5959-5962.

CHAPTER II

EXPERIMENTAL AND ANALYTICAL METHODS

Introduction

Several methods of characterization are employed in this work to enable analysis of films and their performance. This chapter introduces these methods and provides insight into their usefulness relative to the work reported in subsequent chapters.

Photosystem I Extraction and Purification

The processes used for the extraction and purification of PSI protein complexes from spinach and kudzu were identical. Reeves and Hall[1] set a standard procedure in 1980, which has been adapted for our laboratory.[2] Organic baby spinach was purchased from the local grocery store chain and stored in the refrigerator a couple of days prior to the extraction process. Kudzu leaves were picked from the side of the road in Macon County, TN the morning of the extraction process. All leaves were de-veined resulting in ~60 grams of leaves, which were homogenized in a blender. After maceration, the mixture was filtered through 2 layers of cheesecloth followed by 8 layers, keeping the receptacle on ice. Once plant cells are ruptured, many proteolytic and other degrading enzymes are released, which can denature the PSI. Conducting all procedures while keeping all solutions cold limit these harmful effects. Expediency in processing is prudent for the same reason. The filtration

results in ~200 mL of a green solution, which is subsequently centrifuged in two steps: i) centrifugation at 8000 RCF for 5 seconds and the supernatant poured off. The pellet is resuspended in buffer and ii) centrifugation at 20000 RCF for 15 minutes producing a dark green supernatant. The protein is purified using a chilled hydroxylapatite column previously described by Shiozawa et al.[3] Aliquots were stored at -80 °C prior to deposition. Upon removal from storage and prior to deposition of the kudzu multilayer films, the PSI solution is subjected to dialysis using 10 kDa Biotech Cellulose Ester dialysis membrane tubing (Fisher Scientific) in 4000 L of deionized water for 24 hours. However, for spinach PSI monolayer films, no dialysis was necessary.

Graphene Synthesis

Graphene films were grown following the work of Ruoff's group,[4] by chemical vapor deposition on 25-μm thick Cu foils cut into thin strips and placed inside a fused silica tube where they were heated using a hot wall furnace. The Cu foil was first heated at 1000 °C under 2 sccm flow of hydrogen, H_2(g) at ~25 mTorr to remove contaminants and oxides from the Cu surface. Subsequently, 35 sccm of CH_4(g) was introduced along with the 2 sccm of H_2 for 30 min, while pressure was maintained at ~250 mTorr. Then the furnace was allowed to cool to room temperature. PMMA (A7) resist was spin-coated onto the samples at 4000 rpm for 45 s, making a PMMA/graphene/Cu sandwich. The Cu was then etched away (APS-100 copper etchant) and the resulting PMMA/graphene stack was placed into a DI water bath where it was transferred onto designated Si/SiO_2, Au or glass substrates.

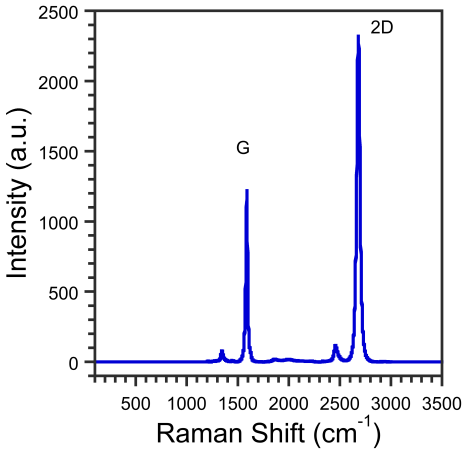

Figure 2. Raman Spectra with G peak intensity of 1240, 2D peak intensity of 2333.

After drying, the PMMA was removed using acetone. Each sample was cut to 1 cm x 1 cm squares with electrical contact made via Cu tape.

Raman spectra were taken to verify the presence of the graphene film. Figure 2 shows the expected peaks with the ratio of G:2D peaks equal to 0.53 and a small D-peak at 1343 cm^{-1}, which is attributed to minor defects in pristine graphene.[5]

Substrate Preparation

Gold (Au) substrates were gold-coated silicon wafers (WRS Materials) prepared by first evaporating a 100 Å layer of chromium followed by ~1250 Å of gold at a base pressure of 5 x 10^{-6} Torr. The Au substrates were then rinsed in ethanol and deionized water and dried in a stream of nitrogen, N_2.

Boron-doped silicon, p-Si, wafers <100> with 525 μm thickness and ≤ 0.01 ohm-cm resistance were bought from University Wafer. These were etched in 2% hydrofluoric acid solution prior to use. *Warning: Hydrofluoric acid is life threatening if absorbed into the body! Refer to MSDS and take appropriate precautions when using this chemical.*

Microscope cover slips (Fisher Scientific) were rinsed in ethanol and deionized water and dried in N_2 gas flow prior to deposition of graphene. Circular masks (Gamry Instruments) were used to define cell areas for each substrate.

Optical Spectroscopy and Analysis

Spectroscopy is the absorption, emission and scattering of electromagnetic radiation by matter measured wavelength-by-wavelength. In optical spectroscopy, the interplay between electromagnetic radiation and matter is monitored in the ultraviolet (UV), visible (VIS) and infrared (IR) region, from 350 nm to 750 nm in this work. As incident photons are absorbed by the material, individual molecules transition from their initial energy state, E_i to an excited final energy state, E_f. According to the conservation of energy, the initial energy less the final energy is equivalent to the energy of the absorbed photon, expressed as $h\nu$, where h is Plank's constant and ν is the frequency of radiation, which is determined by dividing c, the speed of light in a vacuum, by the wavelength.

$$\Delta E = E_i - E_f = h\upsilon = h\frac{c}{\lambda} \quad (1)$$

When the molecule transitions from the excited state to a lower state emitting a photon, this is called fluorescence (emission). When a photon travels into a material and becomes scattered, it can be classified as Rayleigh scattering, where the scattered radiation is at the same frequency as the initial radiation (elastic scattering), or Raman scattering, where the scattered radiation varies in frequency (inelastic scattering). Raman scattering is due to the effects of vibrational, rotational

or electronic energy of a molecule. Raman spectra are useful in determining the presence of graphene on a substrate in this work.

Collecting the UV-vis spectrum of a PSI film deposited on a UV-vis-transparent graphene/glass substrate enhanced the study of the composition. A Varian Cary 5000 UV-VIS-NIR spectrophotometer was used in this work. Additionally, UV-vis spectroscopy was used for the determination of PSI concentration in solution, which follows the Beer-Lambert law that states the absorption of light, A is equivalent to the negative logarithm of the ratio of the intensity transmitted, I to the intensity incident on the sample, I_o. This is further explained as the optical path length, l, times the concentration, c, times the extinction coefficient, ε.

$$A = -log\left(\frac{I}{I_o}\right) = \varepsilon * c * l \quad (2)$$

The P_{700} concentration was determined by measuring the ferricyanide-oxidized minus the ascorbate-reduced difference spectrum using the difference extinction coefficient of 64 mM^{-1} cm^{-1} for the red absorbance minima (around 700 nm) with respect to the isosbestic point at 725 nm.[6] The reaction mixture contained the following: 50 mM Tricine, 0.1 M Sorbitol, 0.01 M NaCl, and 0.05% Triton X-100 in 100 mL water adjusted to pH 7.8 with NaOH. For the reduction of P_{700}, a mixture of 0.5 M sodium ascorbate and 5 mM dithiothreitol (DTT) was added to the reference cuvette, and for oxidation, 1 M potassium ferricyanide was added to sample cuvette. PSI in higher plants is not known to form trimers and P_{700} is distributed as one per PSI complex. Therefore, the concentration of P_{700} is equivalent to the concentration of PSI.

In order to determine the concentration of chlorophyll *a* and *b,* denoted as chl *a* and chl *b*, absorbance data were collected at wavelengths of 645 and 664 nm. These data were used in Porra's set of equations[7] as follows:

$$[chl\ a] = 13.71\ A^{664} - 2.85\ A^{645} \quad (3)$$

$$[chl\ b] = 22.39\ A^{645} - 5.42\ A^{664} \quad (4)$$

$$[chl\ a + b] = 19.54\ A^{645} + 8.29\ A^{664} \quad (5)$$

Porra determined these equations for buffered aqueous, 80% acetone solvent. The absorbance variables, A^{λ} represent the data collected at a wavelength of λ with results in [nmol/ml].

In order to investigate the surface composition, polarized modulation infrared reflectance-absorption spectroscopy (PM-IRRAS) data were collected on the Bruker Tensor 27 equipped with PMA 50. The spectrometer is also equipped with the Seagull variable angle reflection accessory for external, diffuse reflection modes and ATR with hemispherical internal reflection elements (ZnSe, Ge). Graphene was transferred to an infrared reflective surface (Au) prior to deposition of PSI. The angle of incidence was 80°.

Additional reflectance-absorbance infrared spectroscopy (RAIRS) measurements of PSI deposited onto Au were taken with a Varian 3100 FT-IR, Excalibur Series spectrometer with Resolutions Pro software (version 4.0.5.009) from Varian, Inc. The RAIRS p-polarized light was incident at 80° from the surface normal. The data were taken in single reflection mode with a liquid-nitrogen cooled, narrow band mercury cadmium telluride detector. Spectral resolution was 2 cm^{-1} after triangular

apodization. Each spectrum was collected over 500 scans with a bare Au substrate as the background. A water spectrum was measured by rescanning the background sample in the presence of water vapor, and it was subtracted from the spectrum of each sample to better resolve the peaks of interest in the 1400 to 2000 cm^{-1} range. Otherwise, the presence of water was minimized by the flow of dry air through the sample compartment.

Spectroscopic Ellipsometry (SE) measurements were obtained on a J. A. Woolham Co. M-2000DI variable angle spectroscopic ellipsometer with CompleteEase™ software for modeling. Measurements were taken at three independent locations per sample at incident angles of 70, 75, and 80 degrees from surface normal and modeled using wavelengths of 400-700 nm. Optical constants were simultaneously measured and verified. For graphene on Si/SiO_2 substrates, the bare Si/SiO_2 was measured and modeled using CompleteEase™ SI JAW substrate with INTR JAW set at 10.00 Å followed by SIO2 JAW fitting the thickness.[8] The final average thickness for fitting the layer was 3004.30 Å in good agreement with the manufacturer's specifications. Graphene measurements were taken and modeled using a Cauchy film as the starting material, parameterized to a B-spline with n = 1.5, k = 0 at a resolution of 0.3 eV, resulting in 18 points. Graphene thickness models varied from the interlayer distance of graphite, which is in agreement with Kravets et al.[9] and possibly results from residuals on the surface. The Raman data were verified for each graphene sample, confirming a monolayer on the surface of both the Si/SiO_2 and glass substrates. There have been several optical ellipsometric studies on graphene, including Gray et al.[10] (3.7 Å) and Weber et al.[11] (3.4 Å). Based

on the analysis by Weber et al., a graphene thickness of 3.4 Å was assumed for subsequent PSI measurements. The PSI was modeled using a Cauchy layer, where A = 1.422, B = 0.002, and C = 0. The measured refractive index was 1.459 at 632.8 nm.

Profilometry

Multilayer film thickness was measured on Veeco Dektak 150 stylus profilometer with a standard scan. The stylus radius was 12.5 μm and the resolution was 0.2 μm/sample. Scan lengths were varied between 2000 to 4500 μm for a duration of 40 to 90 seconds.

Analytical Electrochemistry

Light-induced chronoamperometric data were collected on CH Instruments CHI 660a electrochemical workstation. A custom three-electrode electrochemical cell with a Ag/AgCl (saturated KCl) reference electrode, a Pt mesh counter electrode and the working electrode of interest was staged inside a Faraday Cage. The electrochemical mediator solutions were chosen according to the experiments being investigated and are included in that discussion. Each mediator solution included 100 mM potassium chloride from Sigma-Aldrich and deionized water, purified with a Modu-Pure system. Remaining details are described in the main text according to the pertinent experiment.

Photochronoamperometric measurements were performed at the open-circuit potential of the system, which was determined experimentally for each sample. Any overpotential used for these measurements are noted in the main text. Illumination was provided by a 250 W cold light source, the Leica KL 2500 LCD. In some

experiments a 633 nm high pass filter was utilized. Light intensity was measured using an analog coherent 210 power meter. The spot area of the detector was 4.9 cm^2. The white light intensity measured 82 mW/cm^2 and the light intensity using the high bypass red filter measured 98 mW/cm^2. The fixtures used for mounting the samples for testing in white light had a longer path length than the fixture holding the samples for testing in red light, decreasing the intensity over that of the red light path length. Sunlight AM 1.5 is typically quoted as 100 mW/cm^2 and this is the generally accepted intensity for calculating efficiencies in this field. When the variance or tolerance factors are included, our lamp intensities coincide with AM 1.5 intensity. The photocurrent values were obtained by measuring the difference in the dark current and the current under illumination at specified time intervals in the main text. Reported error bars represent the standard deviation of the samples included in the study and noted in the text. Cyclic voltammogram measurements at a scan rate of 40 mV/s were obtained by measuring the current of the system while scanning a range of voltages in the dark.

References:

1. Reeves, S. G.; Hall, D. O., [8] Higher plant chloroplasts and grana: General preparative procedures (excluding high carbon dioxide fixation ability chloroplasts). In *Methods in Enzymology*, Anthony San, P., Ed. Academic Press: 1980; Vol. Volume 69, pp 85-94.
2. Ciobanu, M.; Kincaid, H. A.; Jennings, G. K.; Cliffel, D. E., Photosystem I Patterning Imaged by Scanning Electrochemical Microscopy. *Langmuir* **2004,** *21* (2), 692-698.
3. Shiozawa, J. A.; Alberte, R. S.; Thornber, J. P., The P700-chlorophyll a-protein : Isolation and some characteristics of the complex in higher plants. *Archives of Biochemistry and Biophysics* **1974,** *165* (1), 388-397.
4. Li, X.; Cai, W.; An, J.; Kim, S.; Nah, J.; Yang, D.; Piner, R.; Velamakanni, A.; Jung, I.; Tutuc, E.; Banerjee, S. K.; Colombo, L.; Ruoff, R. S., Large-Area Synthesis of High-Quality and Uniform Graphene Films on Copper Foils. *Science* **2009,** *324* (5932), 1312-1314.

5. Ferrari, A. C.; Meyer, J. C.; Scardaci, V.; Casiraghi, C.; Lazzeri, M.; Mauri, F.; Piscanec, S.; Jiang, D.; Novoselov, K. S.; Roth, S.; Geim, A. K., Raman Spectrum of Graphene and Graphene Layers. *Physical Review Letters* **2006,** *97* (18), 187401.
6. Baba, K.; Itoh, S.; Hastings, G.; Hoshina, S., Photoinhibition of Photosystem I electron transfer activity in isolated Photosystem I preparations with different chlorophyll contents. *Photosynthesis Research* **1996,** *47* (2), 121-130.
7. Porra, R. J., The chequered history of the development and use of simultaneous equations for the accurate determination of chlorophylls a and b. *Photosynthesis Research* **2002,** *73* (1-3), 149-156.
8. J.A. Woollam Co., I., CompleteEase Data Analysis Manual. Lincoln, NE, 2004-2011; pp. 51-58.
9. Kravets, V. G.; Grigorenko, A. N.; Nair, R. R.; Blake, P.; Anissimova, S.; Novoselov, K. S.; Geim, A. K., Spectroscopic ellipsometry of graphene and an exciton-shifted van Hove peak in absorption. *Physical Review B* **2010,** *81* (15), 155413.
10. Gray, A.; Balooch, M.; Allegret, S.; De Gendt, S.; Wang, W. E., Optical detection and characterization of graphene by broadband spectrophotornetry. *Journal of Applied Physics* **2008,** *104* (5).
11. Weber, J. W.; Calado, V. E.; van de Sanden, M. C. M., Optical constants of graphene measured by spectroscopic ellipsometry. *Applied Physics Letters* **2010,** *97* (9), 091904.

CHAPTER III

Photosystem I on Graphene as a Highly Transparent, Photoactive Electrode

Introduction

PSI derived from spinach is a 500-kDa complex composed of 17 proteins.[1] As mentioned in the introduction, these protein complexes can be extracted from plants to serve as photodiodes in an electrical circuit. In this chapter, we demonstrate the ability to adsorb PSI extracted from spinach onto highly transparent graphene (97%). The transparency of graphene supports the choice of an opaque mediator at elevated concentrations, which enables the report herein of 550 nA/cm^2 photocurrent from a monolayer of PSI on graphene in the presence of 20 mM methylene blue, which yields an opaque blue solution. The PSI-modified graphene electrode has a total thickness of less than 10 nm and demonstrates photoactivity that is an order of magnitude larger than that for unmodified graphene, establishing the feasibility of conjoining these nanomaterials as potential constructs in next-generation photovoltaic devices.

Materials and Methods

PSI complexes were extracted from commercial baby spinach as described in Chapter I. After UV-vis characterization, the PSI concentration was determined as 3.2 mM. The extracted PSI was directly deposited as monolayer films onto

graphene-coated silicon, gold, and glass substrates by the vacuum-assisted, drop-casting method[2] developed within our group.

Results and Discussion

Spectra were collected to analyze the surface composition of PSI monolayer films prepared on graphene. Figure 3a shows the polarized modulation infrared reflectance-absorption spectroscopy (PM-IRRAS) revealing Amide I and Amide II peaks at ~1662 cm^{-1} and ~1540 cm^{-1}, respectively, indicative of the protein complex.[3] Additionally, UV-vis spectra shown in figure 3b revealed two distinct peaks at ~680 nm and ~440 nm, consistent with the chlorophylls of PSI[4] present on the surface of the graphene electrode. Together, the PM-IRRAS and the UV-vis spectra indicate that PSI is adsorbed onto the graphene surface.

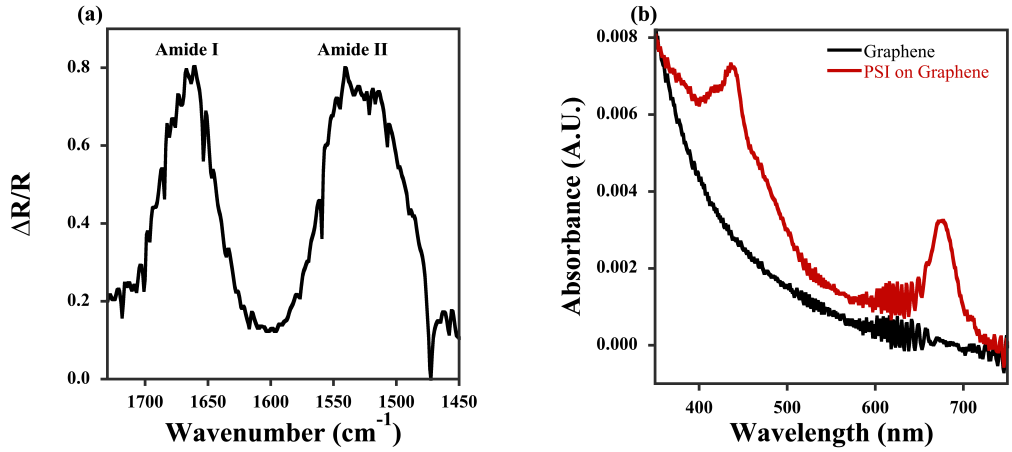

Figure 3. Spectroscopic analysis of PSI-modified graphene electrodes. a) PM-IRRAS spectrum of a PSI film deposited onto a graphene/Au electrode. The absorbance values at 1662 cm^{-1} and 1540 cm^{-1} correspond to the Amide I and II stretches respectively.[3] b) UV-vis absorbance spectrum of an unmodified graphene electrode (black) and PSI film deposited on graphene/glass electrode (red). The absorbance of the glass was subtracted from the measurements, and the value for the absorbance at 750 nm was set to zero in order to easily observe the absorbance change between the unmodified and PSI-modified graphene. The two distinct peaks at ~680 nm and ~440 nm are consistent with the chlorophylls of PSI.[4]

Ellipsometric thicknesses of the PSI films were measured to assess the coverage of protein deposited on the graphene substrate. The average thickness measurement for PSI films was 58 Å with a standard deviation of ± 15 Å, using a Cauchy model. Based on the reported size of PSI[5] and the considerable free volume contained in a complete monolayer of PSI in which the proteins are oriented with their electron transfer vectors normal to the substrate, we estimate that a complete monolayer would yield an ellipsometric thickness of ~80 Å, which agrees well with the greatest thicknesses reported for PSI monolayers.[2] Therefore, a measurement of 58 Å represents approximately 70% surface coverage of PSI on the graphene surface.

To further investigate the effective coverage of PSI on the electrode, electrochemical experiments were performed in the dark to assess the ability of the PSI film to block the access of redox-active species to the underlying graphene. Figure 4 shows cyclic voltammograms (CV) recorded in the absence of light, where the applied potential to the working electrode was cycled from -0.35 to 0.05 V vs. Ag/AgCl in the presence of ruthenium hexamine trichloride (RuHex) as the current was measured continuously. The underlying substrate (SiO_2) acts as an insulator so that no current is observed at any potential. The unmodified-graphene substrate reveals an increasing current as the voltage sweep becomes more negative, which is attributed to reduction of the $[Ru(NH_3)_6]^{3+}$ species. As the voltage sweeps more positive, an oxidation peak appears at -0.1 V, which is the expected formal potential (versus Ag/AgCl) of the $[Ru(NH_3)_6]^{2+}$ species,[6] demonstrating that the graphene

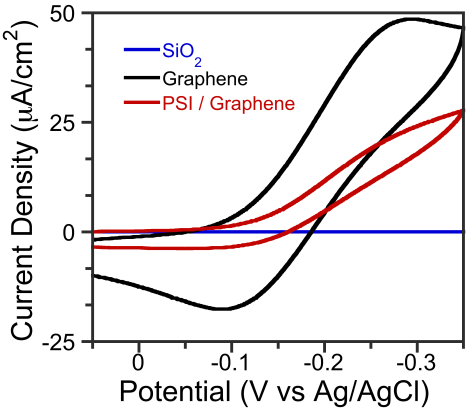

Figure 4. Cyclic voltammograms of the SiO_2 substrate (blue), unmodified graphene electrode (black), and PSI-modified graphene electrode (red), taken in the dark, using ruthenium hexamine trichloride (2 mM) in aqueous phosphate buffer (5 mM) solution with potassium chloride (0.1 M). The potential of the working electrode was scanned from -0.35 to 0.05 V vs. Ag/AgCl at a rate of 0.1 V/s.

film is conductive and an appropriate electrode for this process. After deposition of a PSI monolayer, the observed reductive and oxidative currents decrease as a result of PSI blocking mediator access to a majority of the electrode surface. Assuming that PSI completely blocks the electrode area that it occupies from mediator interaction, a PSI surface coverage of ~70% was estimated from the decrease in integrated charge for the reduction peak after adsorption of PSI, consistent with that gleaned from ellipsometric measurements.

Photochronoamperometric analyses of PSI-modified graphene electrodes were performed to determine their photocurrent activity and to compare the results with unmodified graphene electrodes. Figure 5a shows the photo-response of the PSI-modified graphene electrode (red) in comparison to an unmodified graphene electrode (black) measured at open-circuit potential. Upon illumination with white light having an intensity of 82 mW/cm^2, an electron is excited from the P_{700} to the F_B site of PSI. The graphene electrode draws the electron from the F_B^- site of PSI and

the $[Ru(NH_3)_6]^{2+}$ mediator reduces the resulting P_{700}^+ site, resulting in a negative photocurrent, or an anodic response. Unmodified graphene is also capable of light-assisted mediator oxidation in the absence of PSI; however, the observed photocurrent is 8-fold lower than that of the PSI-modified electrode. Changing the potential of the electrode can change the direction of electron flow (Figure 5b). When -100 mV overpotential is applied to the electrode, the ability for the electrode to give up electrons increases so that photo-reduction of P_{700}^+ and the oxidized mediator are observed as positive or cathodic photocurrent. The "saw-tooth" shape of this curve is consistent with a diffusional response of the mediator to the additional reducing ability of the PSI/graphene electrode in the light. Additionally, the photocurrent observed is significantly higher than when the system is at open-circuit potential or at a positive overpotential. The fact that photocurrent switches

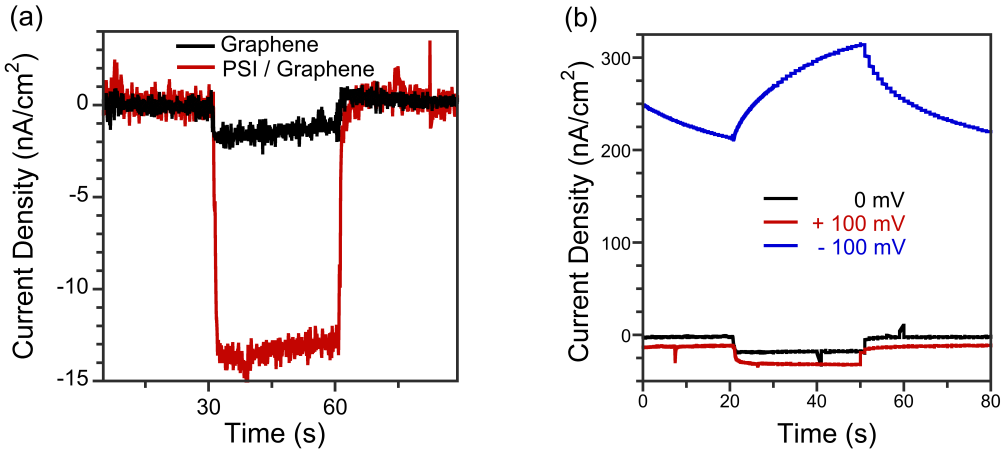

Figure 5. Photochronoamperometric analyses of PSI-modified graphene electrodes. All measurements were made using ruthenium hexamine (0.2 mM), potassium chloride (0.1 M), and phosphate buffer (5 mM) as the mediator solution. White-light at an intensity of 82 mW/cm^2 was irradiated onto the surfaces for 30 s. a) Comparison between an unmodified graphene electrode (black) and a PSI-modified graphene electrode (red). Both samples were measured while holding the working electrode at the open circuit potential. The light was on from 30 s to 60 s. b) Comparison of a PSI-modified graphene electrode held at 0 mV or open-circuit potential (black), a positive 100 mV overpotential (red), or a negative 100 mV overpotential (blue). The light was on from 20 s to 50 s.

from anodic to cathodic suggests that PSI is deposited onto graphene in different orientations, which produce electron transfer vectors leading both to and from the graphene surface, yielding photocurrent that reflects a net average of the overall processes occurring at the electrode surface held at a constant potential. Importantly, these results show that applied potential can be used to direct the flow of current between graphene and the PSI film.

One benefit of using graphene as a transparent, conducting electrode is the flexibility it allows with mediator choice and concentration. For example, by mounting graphene on glass, we can irradiate the cell through the transparent graphene electrode rather than through the solution, enabling the use of opaque mediators at higher concentrations to boost photocurrents.[6] Figure 6 shows a photochronoamperometry experiment where we have used methylene blue (MB) as an opaque, redox-active mediator and red light with an intensity of 98 mW/cm^2. MB has not been used with more traditional electrodes because it absorbs in the red regime (650-750 nm) where it deprives PSI of incident photons that would be absorbed by the chlorophyll network of PSI (Figure 3b). Figure 6 shows the results of measured photocurrent taken through the opaque mediator (blue), compared to the measured photocurrent taken through the graphene substrate for both PSI-modified (red) and unmodified graphene (black). The absence of photocurrent confirms absorption of light by the mediator when the light initially passes through the solution on its path to the PSI-modified or unmodified graphene substrate. In contrast, the photocurrent measured when the light passes through the transparent graphene electrode first (~550 nA/cm^2) confirms that photons are absorbed by PSI,

initiating the measured photoresponse, which is highly complex and diffusional based on the time-dependence of the local concentration of MB at the electrode. Similar to the previous electrochemical measurements in transparent RuHex, the graphene was able to reduce the mediator in the absence of PSI. The PSI-modified graphene electrode shows a 10-fold enhancement over the bare graphene electrode at 20 s after irradiation in this case. The effect of mediator concentration on current density is shown in Figure 6b. The current density for these PSI-modified graphene electrodes increased by a factor of 20 as the MB mediator concentration increased from 0.2 to 20 mM. Here, the integration of PSI monolayer films with graphene as an atomically thin, transparent electrode enables the achievement of these high

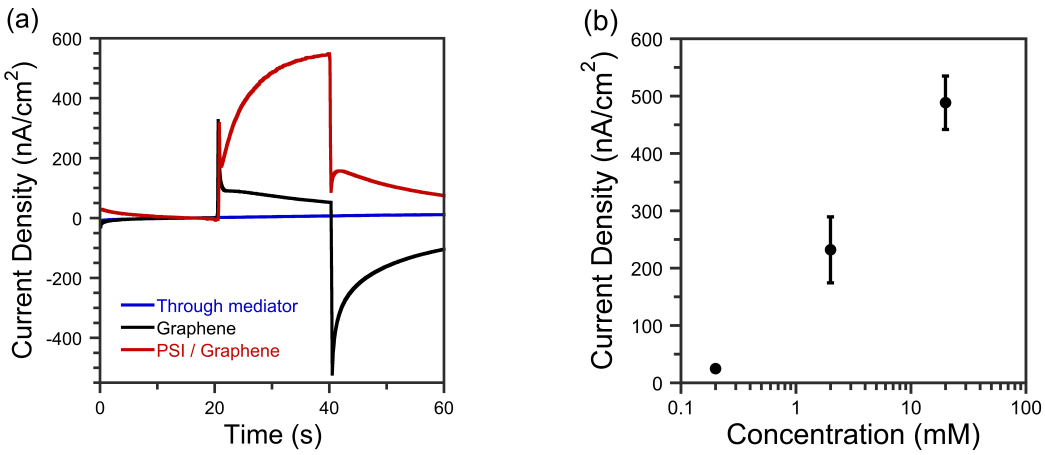

Figure 6. a) Photochronoamperometric analysis of a PSI-modified graphene electrode on glass (red) as compared to an unmodified graphene electrode (black) irradiated through the electrode and compared to electrodes irradiated through the mediator (blue). All measurements were made using 20 mM MB aqueous mediator with 0.1 M KCl. Irradiance using a 633 nm filter resulting in 98 mW/cm^2 intensity was supplied at 20 s and removed at 40 s for each measurement. b) The effect of MB mediator concentration on the measured photocurrent density, measured 20 s after turning on the light. Error bars reflect standard deviation from 6 samples. If no error bar is present, the size of the symbol reflects the error.

photocurrents, whereas traditional opaque electrodes would not allow testing under these conditions. This unique system, combined with the reported long-term stability[7] and enhanced performance of thicker PSI films[8] offers exciting opportunities to amplify biohybrid cell performance.

Conclusions

We have demonstrated the adsorption of PSI monolayers directly onto graphene electrodes for the conversion of light to electrical current. This system provides a photoelectrochemical response to irradiation as measured in an electrochemical cell that can be enhanced with the use of overpotential. The transparent nature of graphene enables use of a highly effective and opaque mediator (MB) to greatly amplify photocurrents. This research represents the first report of integrating PSI with atomically thin graphene to create a photoactive biohybrid electrode thinner than 10 nm. This work establishes a foundation for exploiting the unique properties of these nanomaterials in future biohybrid devices.

References:

1. Amunts, A.; Drory, O.; Nelson, N., The structure of a plant photosystem I supercomplex at 3.4 A resolution. *Nature* **2007,** *447* (7140), 58-63.
2. Faulkner, C. J.; Lees, S.; Ciesielski, P. N.; Cliffel, D. E.; Jennings, G. K., Rapid Assembly of Photosystem I Monolayers on Gold Electrodes. *Langmuir* **2008,** *24* (16), 8409-8412.
3. Yada, L. D. S., *Organic Spectroscopy*. Kluwer Academic Publishers: New Delhi, 2005; p 324.
4. Baba, K.; Itoh, S.; Hastings, G.; Hoshina, S., Photoinhibition of Photosystem I electron transfer activity in isolated Photosystem I preparations with different chlorophyll contents. *Photosynthesis Research* **1996,** *47* (2), 121-130.
5. Amunts, A.; Toporik, H.; Borovikova, A.; Nelson, N., Structure Determination and Improved Model of Plant Photosystem I. *J Biol Chem* **2010,** *285* (5), 3478-3486.
6. Bard, A. J.; Faulkner, L. R., *Electrochemical Methods: Fundamentals and Applications*. 2nd ed.; John Wiley & Sons, Inc.: New York, 2001.

7. Ciesielski, P. N.; Hijazi, F. M.; Scott, A. M.; Faulkner, C. J.; Beard, L.; Emmett, K.; Rosenthal, S. J.; Cliffel, D.; Kane Jennings, G., Photosystem I - Based biohybrid photoelectrochemical cells. *Bioresource Technology* **2010,** *101* (9), 3047-3053.
8. Ciesielski, P. N.; Faulkner, C. J.; Irwin, M. T.; Gregory, J. M.; Tolk, N. H.; Cliffel, D. E.; Jennings, G. K., Enhanced Photocurrent Production by Photosystem I Multilayer Assemblies. *Adv Funct Mater* **2010,** *20* (23), 4048-4054.

CHAPTER IV

Pueraria lobata (Kudzu) Photosystem I Improves the Photoelectrochemical Performance of Silicon

Introduction

In prior work, our group has successfully extracted PSI protein complexes from spinach leaves and deposited them on various substrates, such as gold, glass, ITO and alumina to investigate "wet" photoelectrochemical cells where diffusible redox mediators transfer electrons between a PSI-coated working electrode and a counter electrode.[1] In 2007, we generated ~4 nA/cm^2 of photocurrent with isolated PSI sub monolayers deposited on Au electrodes.[2] The following year, we developed a rapid assembly approach to achieve dense PSI monolayers, which resulted in ~100 nA/cm^2 of photocurrent,[3] and we later incorporated nanoporous gold electrodes to increase the PSI/electrode interfacial area, reaching ~300 nA/cm^2.[4] Further studies led our group to investigate thick multilayers of this exciting protein on Au substrates, achieving ~10 mA/cm^2 of photocurrent in 2010.[5] The persistent challenge of PSI orientation relative to the substrate and within the film's multilayers was very recently solved through band-gap engineering using p-Si substrates, PSI from spinach leaves, and 0.2 M concentration of methyl viologen, reporting an average photocurrent of ~875 μA/cm^2 for ~1 μm thick films.[6]

Demand for molecular electronics is on the rise opening the door to a vast array of opportunities for biohybrid devices, such as sensors and photovoltaic devices. PSI is an abundant biological resource that is both economical and robust, making it an attractive protein-supramolecular complex for these devices. Conventional electronics cannot match the density of the molecular circuitry found in photosynthetic complexes.[7] In this chapter, an important strategy is to investigate a transition from PSI extracted from spinach to non-traditional food sources, such as kudzu, while taking advantage of the band-gap alignment mentioned above.

Materials and Methods

PSI complexes were extracted from handpicked kudzu leaves as described in Chapter I. After UV-vis characterization, the PSI concentration was determined to be 3.4×10^{-7} M, which is an order of magnitude lower than the average concentration reported for spinach-extracted PSI in our group.[1] Additionally, the ratio of P_{700}:chl *a* is low (89). Typical ratios around 200 are expected.

Prior to deposition, 1 mL of PSI solution was dialyzed in 4 L of deionized water using 10,000 kDa membrane dialysis tubing. This reduced the concentrations of salt and surfactant in the solution. When this aqueous solvent is removed from the dialyzed PSI solution via the vacuum-assisted deposition process, the hydrophobic regions of PSI complexes that were previously stabilized by surfactant seek stabilizing interactions with the hydrophobic regions of other PSI complexes in the film, forming a dense multilayer.

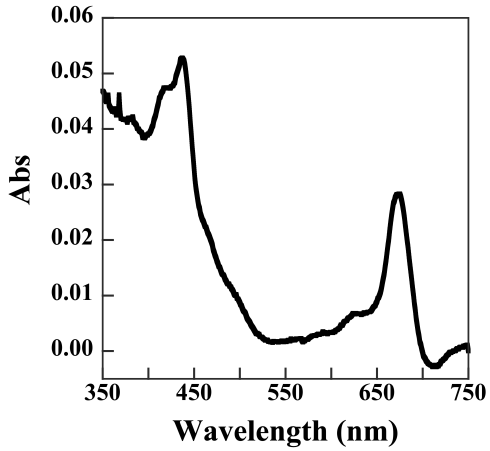

Figure 7. UV-vis spectrum of the characteristic absorbance peaks for PSI extracted from kudzu, in 0.2 M phosphate buffer (pH 7.0) with 0.05% (wt/vol) TritonX-100.

Results and Discussion

After completing the extraction of PSI from kudzu leaves, UV-vis spectrum was measured to verify the solution composition. Characteristic peaks at ~440 nm and ~680 nm in Figure 7 are consistent with the chlorophylls of PSI.

Films of PSI complexes were prepared simultaneously on silicon and gold surfaces by depositing 30 μL of the PSI solution into a well-defined area, applying a vacuum of ~30 mTorr for 10 min, and repeating 12 times. Profilometry measurements provided an average thickness of 0.59 mm with a standard deviation of 0.29 mm across the surface. A RAIRS spectrum of the PSI film on gold was collected to identify the dominant compositional groups from the protein complex. The reflective Au surface was necessary to provide good reflectance signals for the accumulation of the spectrum. Figure 8 shows the Amide I and Amide II peaks at 1664 cm^{-1} and 1546 cm^{-1}, respectively. These peaks represent the amide carbonyl

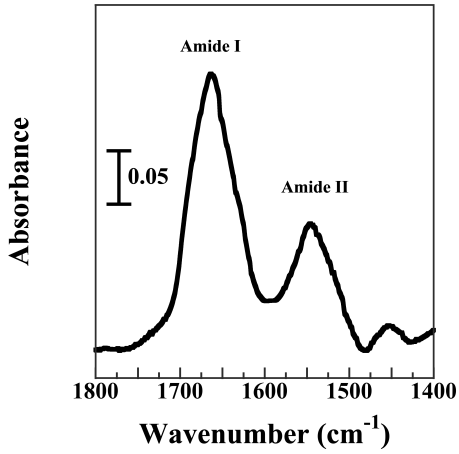

Figure 8. Reflectance absorption infrared spectrum of the Amide I and II peaks at 1664 and 1546 cm^{-1} respectively, for a 0.9 mm thick PSI film deposited on Au.

stretching and the NH bending,[8] respectively, confirming the presence of the protein on the surface.

Photochronoamperometry was performed to measure the ability of the protein to remain photoactive in this cast film out of its native environment. When PSI is irradiated, the chlorophylls absorb the incident photons and transfer them to the P_{700} chlorophyll dimer, which becomes excited and quickly releases an electron, becoming P_{700}^{+}. The electron travels down the electron transfer chain to the F_B (iron-sulfur) site, located on the stromal side of the complex, reducing it to F_B^{-}.[9] In our design, the soluble mediator, methyl viologen, then oxidizes F_B^{-} and transfers the electron to the platinum counter electrode. Meanwhile, the valence band of the p-Si releases an electron to the P_{700}^{+} site, and the cycle repeats as long as sufficient irradiation and mediator are present.

The measurements of current at open-circuit potential are shown in Figure 9. These measurements were taken with the cell isolated in the dark for 30 s, irradiated 30 s, and again measured in darkness (30s to 60s irradiation). The bare p-

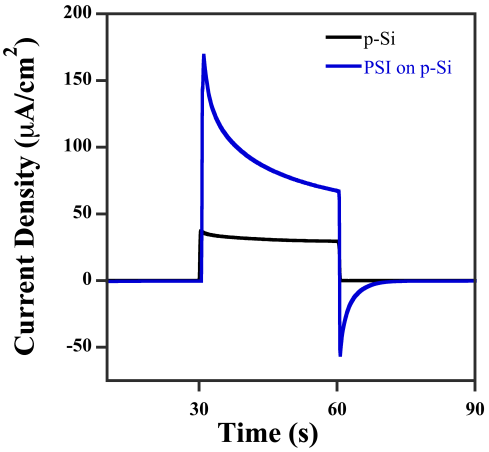

Figure 9. Photochronoamperometric measurements of bare p-Si control and a PSI film deposited on p-Si in a 'wet' electrochemical cell with 20 mM methyl viologen trichloride hydrate and 0.1 M potassium chloride in aqueous solution.

Si working electrode responds to irradiation with a measured current density of ~29 mA/cm^2, while the current density of PSI on p-Si measures ~67 mA/cm^2. This response confirms photocurrent enhancement from the PSI-modified p-Si electrode. The enhancement observed in the presence of the PSI film is due to band gap alignment between the p-Si (valence band energy = 0.5 V vs. NHE) and the PSI reaction center, P_{700} (0.43 V vs. NHE), and the F_B^- site (-0.58V vs NHE) and the redox mediator's formal potential (-0.45 V vs NHE)[6]. In this system, the electrons flow in one direction, from the silicon to the P_{700} site, where they are excited and transferred to the F_B site, and transported by the redox mediator to the counter electrode. Using the same conditions, the kudzu PSI film deposited on Au achieved photocurrent of ~9 mA/cm^2, 4-5-times lower than that of the PSI film on p-Si. Opposite PSI orientations that occur during deposition can result in current cancellation on metal electrodes,[10] whereas enhancement in photocurrent for the

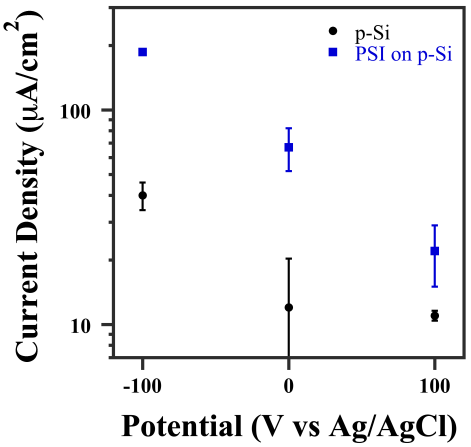

Figure 10. Effect of applied bias on the photocurrent measured for bare p-Si control (black) and a PSI film deposited on p-Si (blue). 0 mV refers to an open-circuit potential of -278 mV and -361 mV for the bare p- Si and PSI film, respectively, vs. Ag/AgCl reference electrode. Error bars represent standard deviation for 5 independently prepared samples per point.

PSI film on p-Si is due to the unidirectional transfer of electrons attributed to the band gap alignment.

Figure 10 shows the influence of applied voltage to the working electrode in these experiments. Adding a negative 100 mV bias to the electrode supplies excess electrons to the circuit. The additional availability of electrons allows the photocurrent in this sample to increase to ~173 mA/cm^2, ~4 times the photocurrent measured for p-Si at this potential (40 mA/cm^2). When the working electrode is biased with positive 100 mV, the photocurrent is repressed by the lack of available electrons. At positive 100 mV bias, the PSI photocurrent of ~22 mA/cm^2 is twice the measured photocurrent in p-Si alone (11 mA/cm^2). These data reflect the aforementioned importance of the band gap alignment in this photoelectrochemical cell.

Conclusions

In conclusion, we have shown that PSI can be extracted from kudzu leaves and deposited as thin films to enhance the photocurrent response of p-Si. Furthermore, these designs can be biased to produce additional photocurrent. Although kudzu is considered a nuisance in the U.S., its rapid growth here, combined with the advancing photoelectrochemical performance of PSI in biohybrid architectures, suggests that many impoverished areas of the world could grow and harvest the leaves of this 'weed' as a means to provide solar power to those who otherwise live without electricity.

References:

1. Ciesielski, P. N.; Faulkner, C. J.; Irwin, M. T.; Gregory, J. M.; Tolk, N. H.; Cliffel, D. E.; Jennings, G. K., Enhanced Photocurrent Production by Photosystem I Multilayer Assemblies. *Adv Funct Mater* **2010,** *20* (23), 4048-4054.
2. Ciobanu, M.; Kincaid, H. A.; Lo, V.; Dukes, A. D.; Kane Jennings, G.; Cliffel, D. E., Electrochemistry and photoelectrochemistry of photosystem I adsorbed on hydroxyl-terminated monolayers. *Journal of Electroanalytical Chemistry* **2007,** *599* (1), 72-78.
3. Faulkner, C. J.; Lees, S.; Ciesielski, P. N.; Cliffel, D. E.; Jennings, G. K., Rapid Assembly of Photosystem I Monolayers on Gold Electrodes. *Langmuir* **2008,** *24* (16), 8409-8412.
4. Ciesielski, P. N.; Scott, A. M.; Faulkner, C. J.; Berron, B. J.; Cliffel, D. E.; Jennings, G. K., Functionalized Nanoporous Gold Leaf Electrode Films for the Immobilization of Photosystem I. *ACS Nano* **2008,** *2* (12), 2465-2472.
5. Ciesielski, P. N.; Hijazi, F. M.; Scott, A. M.; Faulkner, C. J.; Beard, L.; Emmett, K.; Rosenthal, S. J.; Cliffel, D.; Kane Jennings, G., Photosystem I - Based biohybrid photoelectrochemical cells. *Bioresource Technology* **2010,** *101* (9), 3047-3053.
6. LeBlanc, G.; Chen, G. P.; Gizzie, E. A.; Jennings, G. K.; Cliffel, D. E., Enhanced Photocurrents of Photosystem I Films on p-Doped Silicon. *Adv Mater* **2012,** *24* (44), 5959-5962.
7. Mershin, A.; Matsumoto, K.; Kaiser, L.; Yu, D. Y.; Vaughn, M.; Nazeeruddin, M. K.; Bruce, B. D.; Graetzel, M.; Zhang, S. G., Self-assembled photosystem-I biophotovoltaics on nanostructured TiO2 and ZnO. *Sci Rep-Uk* **2012,** *2*, 234-240.
8. Yada, L. D. S., *Organic Spectroscopy*. Kluwer Academic Publishers: New Delhi, 2005; p 324.
9. Golbeck, J. H., Structure and Function of Photosystem I. *Annual Review of Plant Physiology and Plant Molecular Biology* **1992,** *43* (1), 293-324.
10. Ciesielski, P. N.; Cliffel, D. E.; Jennings, G. K., Kinetic Model of the Photocatalytic Effect of a Photosystem I Monolayer on a Planar Electrode Surface. *J Phys Chem A* **2011,** *115* (15), 3326-3334.

CHAPTER V

Summary

This work has further demonstrated the versatility of PSI. For the first time, PSI has been deposited onto graphene. The PSI-modified graphene electrodes provide enhanced photocurrents beyond those of bare graphene. The robust versatility of highly transparent graphene has shown potential for use with a wide range of electrolytes, including opaque mediators, which will further enhance photocurrents. Also for the first time, PSI has been extracted from kudzu, a fast-growing member of the pea family. Although the process remains to be optimized, this work demonstrates the opportunity to utilize a heretofore nuisance in kudzu and utilize it as a productive, renewable resource that could be exploited for commercial use.